

Addressing the Real-world Class Imbalance Problem in Dermatology

Wei-Hung Weng*
MIT

CKBJIMMY@MIT.EDU

Jonathan Deaton
Google Health

JDEATON@GOOGLE.COM

Vivek Natarajan
Google Health

NATVIV@GOOGLE.COM

Gamaleldin F. Elsayed
Google Research

GAMALELDIN@GOOGLE.COM

Yuan Liu
Google Health

YUANLIU@GOOGLE.COM

Abstract

Class imbalance is a common problem in medical diagnosis, causing a standard classifier to be biased towards the common classes and perform poorly on the rare classes. This is especially true for dermatology, a specialty with thousands of skin conditions but many of which have rare prevalence in the real world. Motivated by recent advances, we explore few-shot learning methods as well as conventional class imbalance techniques for the skin condition recognition problem and propose an evaluation setup to fairly assess the real-world utility of such approaches. When compared to conventional class imbalance techniques, we find that few-shot learning methods are not as performant as those conventional methods, but combining the two approaches using a novel ensemble leads to improvement in model performance, especially for rare classes. We conclude that the ensemble can be useful to address the class imbalance problem, yet progress here can further be accelerated by the use of real-world

evaluation setups for benchmarking new methods.

Keywords: Dermatology, Class imbalance, Few-shot learning, Classification.

1. Introduction

Skin disease is the fourth leading cause of non-fatal medical conditions burden worldwide (Seth et al., 2017). Due to the global shortage of dermatologists, access to dermatology care is limited, leading to rising costs, poor patient outcomes, and health inequalities. Recent research endeavors have demonstrated that deep learning systems built to detect skin conditions from either dermatoscopic or digital camera images can achieve expert level performance in diagnosing certain skin conditions (Esteva et al., 2017; Liu et al., 2020). Despite the encouraging progress, such systems can only identify a few common skin conditions well, leaving a vast number of skin conditions still unaddressed in the real-world (Figure 1 (a)).

As many skin conditions occur infrequently in real-world, datasets collected from a natural patient population are highly im-

* Work done at Google.

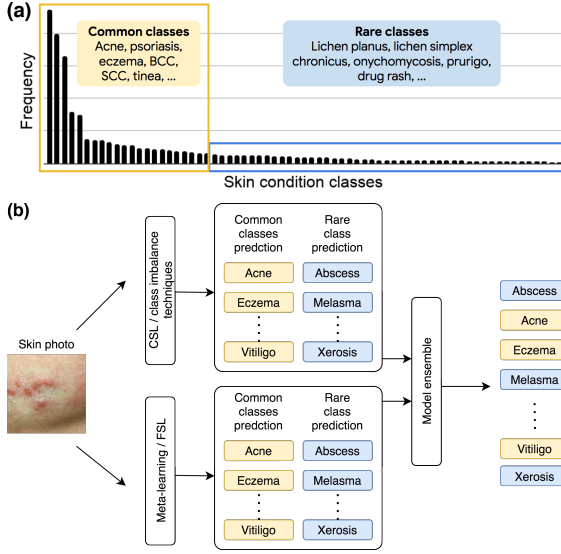


Figure 1: Class imbalance problem in dermatology at a glance (a) and proposed modeling framework (b).

balanced, with few examples for those skin conditions. This makes it challenging to build models that can reliably detect rare skin conditions. Such limitations not only may diminish the clinical utility of these systems due to the low skin condition coverage, but also may cause harm to patients as they are often biased towards common diseases.

A wide variety of techniques have been proposed over the years to address the class imbalance problem in machine learning. These include relatively classic approaches like modified resampling strategies (Chawla et al., 2002), loss reweighting (Eban et al., 2017), focal loss and bias initialization (Lin et al., 2017), to more complex approaches such as using generative models to augment the rare classes with synthetic images (Ghorbani et al., 2020).

A related counterpart to the class imbalance problem is *few-shot learning* (FSL), a learning scenario inspired by the human ability to learn from very few examples (Lake et al., 2011). It can further be generalized to the meta-learning framework that

aims to gain learning experiences from solving many meta tasks in order to achieve a better performance for the tasks (in this case, rare classes) with limited training examples (Vinyals et al., 2016).

The classic evaluation framework for FSL follows an “ N -way- k -shot” setting: given k training examples for N classes as a random subset of all classes, test if the FSL techniques can correctly distinguish among the N classes. It is often not understood whether FSL will translate well beyond this contrived setting to the *real-world* problem, when the task requires recognizing the correct class among *all* possible classes (all-way classification) in the wild (Chen et al., 2019; Triantafillou et al., 2019). Furthermore, it is challenging to compare the classification performance between FSL and the conventional supervised training without a unified evaluation framework.

In this paper, we investigate various FSL methods to tackle the class imbalance problem in skin condition classification (Figure 1 (b)). We modify the typical FSL evaluation setup to adapt to the real-world setting, and design studies to compare FSL methods to *conventional supervised learning* (CSL) with various class imbalance techniques, motivated by the hypothesis that a combination may provide independent predictions, capturing different aspects of the data. Specifically, our contributions are:

- We propose a real-world evaluation framework to compare the FSL methods against conventional methods (i.e., CSL with class imbalance techniques) for the class imbalance problem.
- We find that FSL methods don’t outperform CSL with class imbalance techniques, yet an ensemble of these two

types can outperform either alone, especially for the rare classes.

2. Related Work

2.1. Class Imbalance

Imbalanced class distribution is common in real-world datasets. For mild class imbalance, machine learning algorithms, such as support vector machines (Cortes and Vapnik, 1995), random forests (Breiman, 2001), and modern deep learning techniques can usually handle such cases relatively well. However, special care is required to manage moderate or extreme imbalance situations (Figure 2), when minority classes constitutes typically less than 20% or 1% in the training data respectively.

Conventional Techniques Researchers have developed various resampling and cost-sensitive learning strategies to improve models under such skewed class distribution settings. Resampling aims to balance the class distribution in the training data by either downsampling common classes or upsampling rare classes. Downsampling may increase variance; thus, upsampling is more commonly used, yet upsampling procedures for extremely imbalanced data may be computationally expensive (Weng et al., 2019).

In contrast, cost-sensitive learning penalizes algorithms by increasing the cost of classification mistakes on the rare classes. It can be implemented in various ways, such as reweighting the losses of specific classes, introducing bias as prior into the classification loss at each class (Lin et al., 2017), or less used approaches such as global objectives (Eban et al., 2017). To prevent the easy examples in the common classes from dominating the gradients during classifier training, the focal loss function is developed (Lin et al., 2017), to not only out-weight the rare classes, but also emphasize the hard examples during training.

Few-shot Learning (FSL) FSL can also be utilized to improve the classification performance for the classes with very few training examples. The FSL algorithms can be categorized into several types: metric-based, optimization-based, and transfer learning-based approaches.

Metric-based FSL learn a representation by learning to compare training examples. Koch et al. (2015) developed the Siamese neural network to compare two examples at the same time with two identical twin networks sharing the same weights. Matching network utilizes the cosine similarity as the distance metric and adopts the long-short term memory (LSTM) network for generating embeddings (Vinyals et al., 2016). Prototypical network, on the other hand, uses the Euclidean distance and convolutional networks to determine the embedding of the class prototypes (Snell et al., 2017). Relation networks further employ the concatenation strategy and relation module to score example similarity (Sung et al., 2018).

Optimization-based FSL aims to learn a set of parameters that allows a meta-learner to quickly adapt to new tasks (Finn et al., 2017). Ravi and Larochelle (2016) designed an LSTM-based meta-learner to replace the stochastic gradient decent algorithm in order to learn a better optimizer. One can also learn a better model initialization for faster task adaptation with less gradient updates (Model-Agnostic Meta-Learning, MAML) (Finn et al., 2017). Others have integrated both metric and optimization-based FSL to further improve the performance (Triantafillou et al., 2019).

Finally, transfer learning tackles the few-shot classification fine-tuning a model pre-trained on a much larger dataset (Chen et al., 2019; Tian et al., 2020). Chen et al. (2019) adopts the training-then-finetuning process for few-shot classification without meta-learning (Baseline++). Recently, Tian

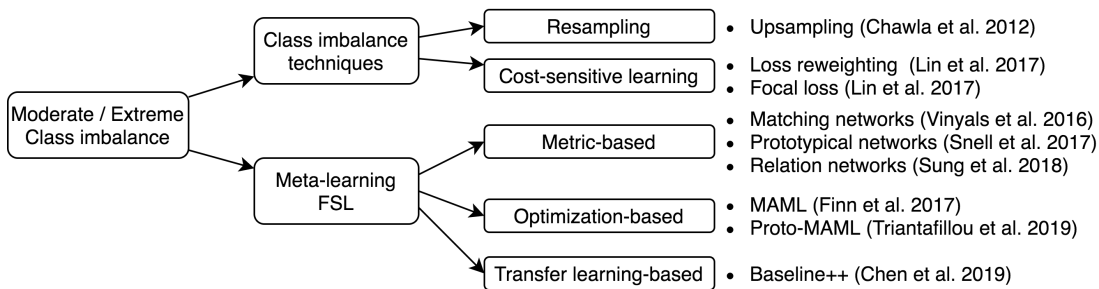


Figure 2: Categories of methods for tackling the class imbalance problem.

et al. (2020) demonstrated that transfer learning under the meta-learning framework can yield strong performance for the few-shot classification problem.

Despite the progress in FSL, they are typically evaluated in a contrived setting and little is known about how they work in real-world all-way classification problems. In this study, we therefore propose an evaluation method that allows us to use FSL for the all-way classification problem, and compare with the CSL-based methods.

2.2. Machine Learning and FSL in Dermatology

Artificial intelligence in dermatology is a rapidly growing topic of interest in recent years (Cruz-Roa et al., 2013; Esteva et al., 2017; Liu et al., 2020; Yang et al., 2018; Prabhu, 2019; Li et al., 2019; Mahajan et al., 2020; Guo et al., 2020; Le et al., 2020). For example, Esteva et al. (2017) applied deep learning to clinical skin photos for two binary skin cancer classification tasks. Liu et al. (2020) developed a CSL-based system that identifies 26 common skin conditions with performance superior to general practitioners and on par with dermatologists.

However, it is challenging to extend such systems to support the rare skin conditions due to the limited training examples. Previous efforts have explored various approaches, such as adopting domain knowledge to learn a better representation (Yang et al., 2018), developing or modifying the meta-learning

based methods (Prabhu, 2019; Li et al., 2019; Mahajan et al., 2020), and making comparison between different approaches tackling the extreme class imbalance problem in dermatology (Guo et al., 2020; Le et al., 2020). Yet there is no study investigating both the FSL and CSL-based class imbalance techniques and comparing them under the real-world all-way classification setting.

Our work focuses on the all-way classification under a extreme long-tailed data distribution that often occurs in real-world medical imaging tasks. Under an unified evaluation framework, we make comparison between FSL and CSL-based class imbalance techniques. We further propose ensembling FSL with conventional methods and demonstrate gains from combining both strategies.

3. Methods

In this work, we investigate the model performance on skin condition classification problem across CSL baseline, CSL with class imbalance techniques, FSL techniques, and different ensembles between these approaches. We use an evaluation setup that allows us to compare across all methods for the real-world classification problem, which entails properly addressing all skin conditions in our datasets. In this section, we explain how we modify the evaluation setup to adapt FSL to this real-world scenario, and introduce the learning algorithms and metrics used for evaluation.

3.1. FSL Task and Evaluation Setup

Task Formulation and Standard Evaluation

FSL follows the meta-learning setting, which consists of training, validation, and testing phases: training for learning a classifier (meta-learner), validation for hyperparameter tuning, and testing for evaluating the learned classifier. Data used in each of the three phases needs to be split into support and query set. For the standard FSL evaluation, the classes used in these three phases should be all disjoint (Figure 3 (a)).

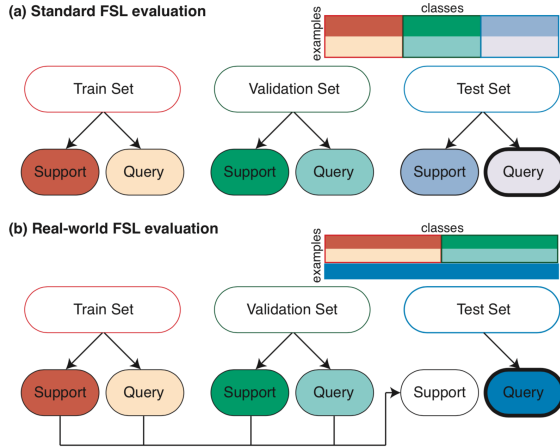


Figure 3: Differences between the standard (a) and the real-world (b) FSL evaluation settings. We report evaluation metrics over the test query sets illustrated with bold box border.

Given a dataset with M classes, the training can be batch or episodic. For batch training, we train a model using all examples from a random N classes ($N < M$) in the train set; for episodic training, we train a classifier under N -way- k -shot learning scenario: in each training episode, we choose random k samples from the random N classes ($N < M$) in the train set to form a support set to learn a model, and then evaluate on a query set which includes other samples in the same N classes in the training set. The validation

and test sets are used to evaluate the model during and after training, respectively.

Real-world Evaluation for FSL The standard N -way- k -shot framework doesn't fit the real-world classification problem, where we need to discriminate all classes simultaneously. Therefore, we introduce the following changes to the classic FSL evaluation setup (Figure 3 (b)): (1) The dataset is split into development (train \cup validation) and test sets in advance, where both sets may contain samples from all possible classes.

(2) Different from the classical setup where the classes in all three splits are disjoint, in the real-world setup, only training and validation have disjoint classes, and both the support set and the query set for those classes come from the development set. During testing, the support set that is used to train the final model comes from the development set, whereas the query set is exactly the same as the test set and includes disjoint samples from *all* classes.

3.2. Modeling

The following FSL algorithms are used in the study (Figure 2): k-nearest neighbors (k-NN) and Baseline++ (Chen et al., 2019), matching networks (Vinyals et al., 2016), prototypical networks (Snell et al., 2017), relation networks (Sung et al., 2018), MAML (Finn et al., 2017) and Proto-MAML (Triantafillou et al., 2019). We also implemented the following CSL-based class imbalance techniques: upsampling with uniform sampling based on the ground truth class during training, bias initialization (BI) with the log of frequency in the training set (Lin et al., 2017), inverse frequency weighting (IFW), focal loss (FL) (Lin et al., 2017), and the combination of BI/IFW and FL/IFW.

3.3. Metrics

We report the balanced accuracy (a.k.a. normalized sensitivity, or macro recall) separately for the common, rare, and all classes for the real-world evaluation. The balanced accuracy is used to account for the class imbalance issue to avoid overweighting the common classes. We also reported the results based on top-1 all-way accuracy in the Appendix. We further report the 95% binomial confidence interval, derived from the mean μ and standard deviation σ of accuracies of E episodes of FSL or E runs of the CSL-based model, which can be expressed as $\mu \pm 1.96 \frac{\sigma}{\sqrt{E}}$.

4. Experiments

4.1. Data

We use the clinical skin images dataset collected by a teledermatology service serving 17 different clinical sites (Liu et al., 2020). We divide the data to different subsets as illustrated in Figure 3 according to the temporal order (75% in the development set and 25% in the test set). Specifically, the test set is chosen to the more recent patient visits, to mimic the real world setting as using earlier data for model training and deploying the model to serve future patients. The development set is further partitioned into train and validation sets based on per skin condition stratified sampling to ensure enough samples for training and validation. The statistics of the data splits are shown in Table A1.

There are a total of 419 skin conditions in the dataset. We define the common classes based on the selection criteria used in (Liu et al., 2020) (more than 100 cases in the development set), and the rare classes as those with (1) more than 20 cases in the development set, and (2) more than 5 cases in the test set. The criteria was established in order to ensure sufficient examples for training and evaluation. For other extremely rare

classes (i.e., classes with ≤ 20 samples in the development set or ≤ 5 samples in the test set) (351 classes), we group them into a single aggregated category “Other” that belongs to a common class due to its sample size. In summary, we have 27 common classes, 42 rare classes (Figure 1 (a), Table A2).

4.2. Training Frameworks

The input for any model is an image of size of 448×448 , and the output is the corresponding skin condition prediction. The Inception-V4 backbone is used for the CSL baseline, and CSL with class imbalance techniques. Inception-V4 is evaluated as the most performant architecture in an internal neural architecture search experiment.

For FSL, we adopt the meta-dataset with the ResNet-18 backbone, which is one of the best performant network architectures in various FSL studies (Triantafyllou et al., 2019; Tian et al., 2020). We train each model using Adam optimizer for 75000 steps with the exponential decay. We follow Triantafyllou et al. (2019) for the learning rate and weight decay setups. We used the batch size of 64 and standard operations like random brightness, saturation, hue, contrast normalization, flip, rotation, and bounding box cropping for data augmentation.

5. Results

We performed experiments to understand (1) whether FSL can be viably applied to the skin condition classification task, (2) how FSL compares against current CSL-based class imbalance techniques, especially on the rare classes, (3) whether combining CSL-based techniques and FSL can further improve the performance across the different skin condition classes.

5.1. Standard FSL Evaluation

In Figure 4 and Table A3, we first benchmark and examine the feasibility of adopting the

standard FSL evaluation (5-way-5-shot classification) to the teledermatology dataset.

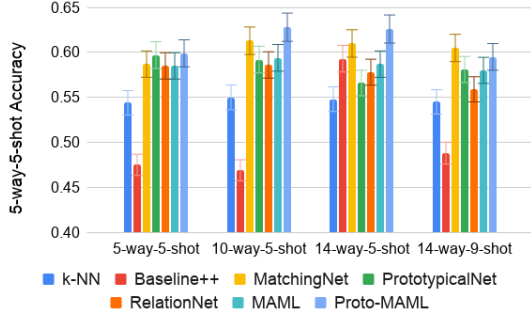


Figure 4: Standard FSL evaluation (5-way-5-shot accuracy with 95% confidence interval) on the teledermatology dataset. We investigate the change of N and k values during training. x-axis is the FSL setting during training.

We find that increasing N yields a trend of better performance. For this particular dermatology use case, a higher way is a relatively optimal option to achieve the best performance under the standard FSL evaluation (Figure 4; N -way-5-shot bars where $N = 5, 10, 14$). However, increasing k is not helpful, possibly because of overfitting (Figure 4; 14-way- k -shot bars where $k = 5, 9$). This finding is consistent with the previous literature (Snell et al., 2017). Among all methods, Proto-MAML and matching networks are comparable and consistently outperforms the others for the teledermatology dataset. This dataset has shown similar properties as other FSL datasets under the standard FSL evaluation.

5.2. Real-world Evaluation

FSL-based Approaches In the real-world setting, we report all-way (69-way) performance (Figure 5, Table A4) on the test set (i.e. query set of the testing phase; see Figure 3 (b)).

The balanced accuracy is chosen as the metric to avoid overweighting the common

classes. We conduct the N -way- k -shot experiments again for finding the optimal training setting under the real-world setup. Different from the findings in the standard FSL evaluation, we find that the optimal N and k values are not quite consistent across methods. The best performant method in the real-world FSL evaluation is also matching networks. In Figure 5 (a, b) and Table A4, we also find that the FSL methods consistently perform better on the rare classes than the common classes.

In brief, we find that the conclusion from the standard FSL evaluation that higher N -way training yields better meta-learner is inconsistent with the real-world evaluation results. Thus, more in-depth exploration is required in real world to identify the optimal N -way setting. We also confirm our hypothesis that the FSL models can be beneficial for rare class prediction but may not be for common classes. For the common class prediction, relying on the CSL methods may be the better option in this case. We later use the top performant models based on validation, which is the matching network model trained in 14-way-9-shot setting, for the model ensemble experiments below.

CSL-based Class Imbalance Techniques Next, we compare the real-world all-way classification performance between FSL methods and CSL-based class imbalance techniques under the single model (non-ensemble) setting. In Figure 6 and Table A5, we find that the best FSL model (matching network) is only slightly better than the CSL baseline for the rare class prediction, possibly because of less training data. Yet the CSL-based class imbalance techniques yield better balance between common and rare classes, as demonstrated with all classes balanced accuracy. Moreover, the CSL-based model integrating focal loss and inverse frequency weighting (FL/IFW) yields even bet-

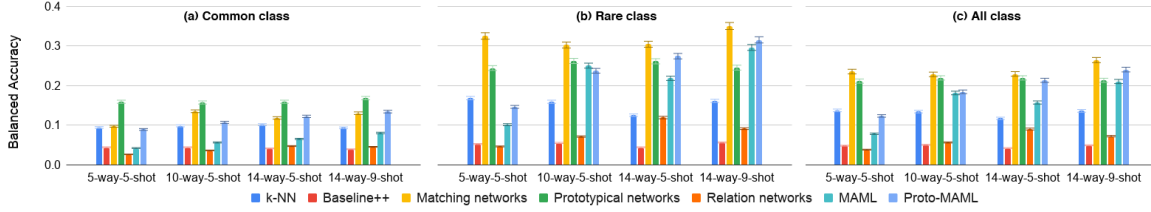


Figure 5: Real-world FSL evaluation. We report the balanced accuracy for (a) common class (b) rare class (c) all class prediction using the models trained by different N -way- k -shot setting.

ter performance on the rare class classification. Such results suggests that FSL is not beneficial when used independently in this real-world setting. One possible explanation could be that given FSL models are not using all the data from common classes during training, it hinders the learning of good low-level visual features for the task, whereas CSL-based models are able to take advantage of it.

where $P_c^{(m)}$ is the probability the m^{th} model in the ensemble gives to class c . We compute the corresponding ensemble logits by first normalizing each model logits ($f_c^{(m)}$) using $\text{LogSumExp}(\cdot)$ (note this normalization does not alter the probabilities) before aggregating the logits from different models:

$$\bar{f}_c = \frac{1}{M} \sum_{m=1}^M (f_c^{(m)} - \log(\sum_{i=1}^C \exp(f_i^{(m)})))$$

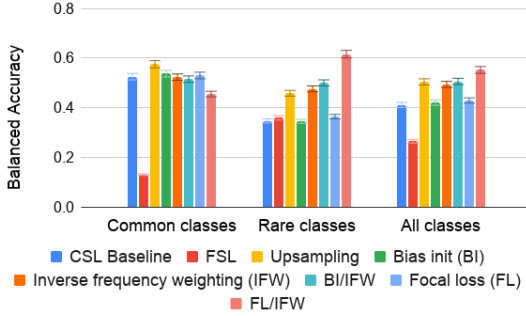


Figure 6: Comparison between FSL and CSL-based class imbalance techniques on the all-way skin condition classification.

Model Ensemble To better utilize the FSL and CSL-based class imbalance techniques, we experiment on ensembling the trained models. We approximate the joint ensemble output probability by computing the geometric mean of the probabilities across M selected models:

$$P_c = \left(\prod_{m=1}^M P_c^{(m)} \right)^{\frac{1}{M}}$$

where \bar{f}_c is the normalized logit for the ensemble. We apply $\text{Softmax}(\cdot)$ to the normalized logits to compute the final ensemble probabilities.

To utilize the CSL-based methods in common class prediction, and FSL in rare class prediction, we further use the prediction from CSL-based methods if the ensemble prediction falls into the group of common classes, and use the prediction from FSL if it is from the group of rare classes while ensembling FSL with CSL-based models. Based on our hypothesis and the results on the validation set, we use the best performant FSL model for rare classes, which is matching network, and the best CSL-based class imbalance model for common classes, which is upsampling method, as basic components for ensemble. In Figure 7 (a) and Table A6, we find that FSL-only ensembles do not perform well, which is consistent with the observations from the previous single model setting. In contrast, ensembling FSL with the CSL-based methods leads to a slight decrease in the common classes yet some improve-

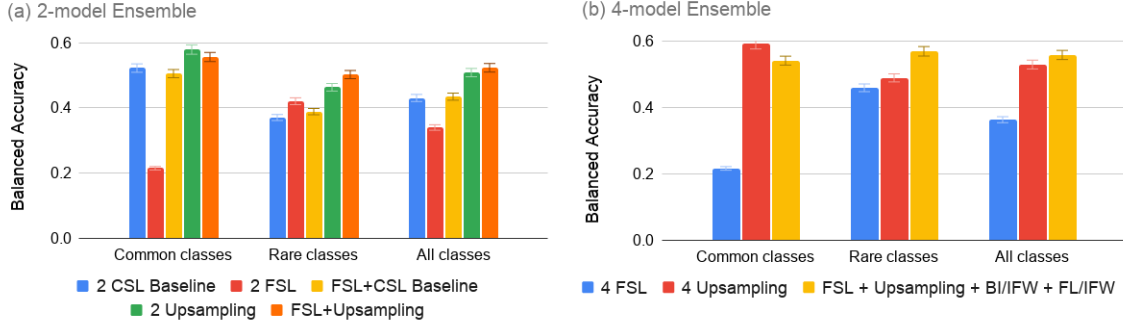


Figure 7: Model ensemble. (a) 2-model ensemble to show the improvement after using FSL. (b) 4-model ensemble to demonstrate the improvement after ensembling models with different mechanisms.

ment over rare classes and all classes in terms of balanced accuracy (Figure 7); ensembling the matching network model with the CSL model with upsampling technique (Figure 7 (a) orange) tends to strike a better balance between common and rare classes. In Figure 7 (b), we find that making the ensemble more heterogeneous by using more models with different mechanisms yields even better trade-off between common and rare classes along with a more notable performance increase, especially for rare classes. These findings confirm our hypothesis that the ensemble of FSL and CSL can be beneficial for such real-world imbalanced skin condition classification problem.

5.3. Qualitative Analysis

In Figure 8, we present eight examples from rare classes alongside with predictions of different models. We show that the FSL and CSL-based class imbalance techniques predict the rare classes more accurately while the CSL baseline tends to be biased toward the common classes such as acne, eczema and psoriasis. For example, eczema is a very common skin condition with various presentations, but it can be visually similar to drug rash or other skin lesions. While the baseline tends to over-predict common classes, the FSL can correctly distinguish the drug rash from eczema or inflicted skin lesions.



Figure 8: Case study of rare classes. FSL and class imbalance techniques are better at identifying rare classes compared to the baseline model.

6. Conclusion

In this work, we propose the real-world evaluation framework to fairly assess and compare the performance between FSL and CSL-based methods on the all-way skin condition classification problem, where extreme class imbalance exists. We find that FSL methods do not outperform class imbalance techniques, yet when ensembled with CSL-based class imbalance techniques, they lead to improved model performance especially for the rare classes. We also observe that ensembling the models with different strengths and more

heterogeneity, such as upsampling and FSL, yields promising results.

To further improve the FSL methods, researchers have, in recent times, proposed stronger representation learning strategies via feature reuse (Raghu et al., 2019), or self-supervised learning (Tian et al., 2020). We believe that evaluating the FSL methods on real-world benchmarks and use cases as the one outlined in this work can greatly accelerate progress in the development of FSL methods with real-world utility.

For future deployment and real-world clinical impact, we also need to account for potential model failures. For example, the false positive cases may lead to wastage of medical resources while the false negative may lead to delayed clinical treatment, especially for malignant cases. The ensemble of both CSL and FSL approaches may mitigate these issues, yet to assess the the generalizability of the results one needs to evaluate our proposed methods on other datasets and domains, which is an interesting future direction of work.

References

- Leo Breiman. Random forests. *Machine learning*, 45(1):5–32, 2001.
- Nitesh V Chawla, Kevin W Bowyer, Lawrence O Hall, and W Philip Kegelmeyer. Smote: synthetic minority over-sampling technique. *Journal of artificial intelligence research*, 16: 321–357, 2002.
- Wei-Yu Chen, Yen-Cheng Liu, Zsolt Kira, Yu-Chiang Frank Wang, and Jia-Bin Huang. A closer look at few-shot classification. *arXiv preprint arXiv:1904.04232*, 2019.
- Corinna Cortes and Vladimir Vapnik. Support-vector networks. *Machine learning*, 20(3):273–297, 1995.
- Angel Alfonso Cruz-Roa, John Edison Arevalo Ovalle, Anant Madabhushi, and Fabio Augusto González Osorio. A deep learning architecture for image representation, visual interpretability and automated basal-cell carcinoma cancer detection. In *International Conference on Medical Image Computing and Computer-Assisted Intervention*, pages 403–410. Springer, 2013.
- Elad Eban, Mariano Schain, Alan Mackey, Ariel Gordon, Ryan Rifkin, and Gal Elidan. Scalable learning of non-decomposable objectives. In *Artificial Intelligence and Statistics*, pages 832–840. PMLR, 2017.
- Andre Esteva, Brett Kuprel, Roberto A Novoa, Justin Ko, Susan M Swetter, Helen M Blau, and Sebastian Thrun. Dermatologist-level classification of skin cancer with deep neural networks. *nature*, 542(7639):115–118, 2017.
- Chelsea Finn, Pieter Abbeel, and Sergey Levine. Model-agnostic meta-learning for fast adaptation of deep networks. *arXiv preprint arXiv:1703.03400*, 2017.
- Amirata Ghorbani, Vivek Natarajan, David Coz, and Yuan Liu. Dermgan: Synthetic generation of clinical skin images with pathology. In *Machine Learning for Health Workshop*, pages 155–170, 2020.
- Yunhui Guo, Noel C Codella, Leonid Karlinsky, James V Codella, John R Smith, Kate Saenko, Tajana Rosling, and Rogerio Feris. A broader study of cross-domain few-shot learning. 2020.
- Gregory Koch, Richard Zemel, and Ruslan Salakhutdinov. Siamese neural networks for one-shot image recognition. In *ICML deep learning workshop*, volume 2. Lille, 2015.

- Brenden Lake, Ruslan Salakhutdinov, Jason Gross, and Joshua Tenenbaum. One shot learning of simple visual concepts. In *Proceedings of the annual meeting of the cognitive science society*, volume 33, 2011.
- Duyen NT Le, Hieu X Le, Lua T Ngo, and Hoan T Ngo. Transfer learning with class-weighted and focal loss function for automatic skin cancer classification. *arXiv preprint arXiv:2009.05977*, 2020.
- Xiaomeng Li, Lequan Yu, Chi-Wing Fu, and Pheng-Ann Heng. Difficulty-aware meta-learning for rare disease diagnosis. *arXiv preprint arXiv:1907.00354*, 2019.
- Tsung-Yi Lin, Priya Goyal, Ross Girshick, Kaiming He, and Piotr Dollár. Focal loss for dense object detection. In *Proceedings of the IEEE international conference on computer vision*, pages 2980–2988, 2017.
- Yuan Liu, Ayush Jain, Clara Eng, David H Way, Kang Lee, Peggy Bui, Kimberly Kanada, Guilherme de Oliveira Marinho, Jessica Gallegos, Sara Gabriele, et al. A deep learning system for differential diagnosis of skin diseases. *Nature Medicine*, pages 1–9, 2020.
- Kushagra Mahajan, Monika Sharma, and Lovekesh Vig. Meta-dermdiagnosis: Few-shot skin disease identification using meta-learning. In *Proceedings of the IEEE/CVF Conference on Computer Vision and Pattern Recognition Workshops*, pages 730–731, 2020.
- Viraj Uday Prabhu. *Few-shot learning for dermatological disease diagnosis*. PhD thesis, Georgia Institute of Technology, 2019.
- Aniruddh Raghu, Maithra Raghu, Samy Bengio, and Oriol Vinyals. Rapid learning or feature reuse? towards understanding the effectiveness of maml. *arXiv preprint arXiv:1909.09157*, 2019.
- Sachin Ravi and Hugo Larochelle. Optimization as a model for few-shot learning. 2016.
- Divya Seth, Khatiya Cheldize, Danielle Brown, and Esther E Freeman. Global burden of skin disease: inequities and innovations. *Current dermatology reports*, 6(3):204–210, 2017.
- Jake Snell, Kevin Swersky, and Richard Zemel. Prototypical networks for few-shot learning. In *Advances in neural information processing systems*, pages 4077–4087, 2017.
- Flood Sung, Yongxin Yang, Li Zhang, Tao Xiang, Philip HS Torr, and Timothy M Hospedales. Learning to compare: Relation network for few-shot learning. In *Proceedings of the IEEE Conference on Computer Vision and Pattern Recognition*, pages 1199–1208, 2018.
- Yonglong Tian, Yue Wang, Dilip Krishnan, Joshua B Tenenbaum, and Phillip Isola. Rethinking few-shot image classification: a good embedding is all you need? *arXiv preprint arXiv:2003.11539*, 2020.
- Eleni Triantafillou, Tyler Zhu, Vincent Dumoulin, Pascal Lamblin, Utku Evci, Kelvin Xu, Ross Goroshin, Carles Gelada, Kevin Swersky, Pierre-Antoine Manzagol, et al. Meta-dataset: A dataset of datasets for learning to learn from few examples. *arXiv preprint arXiv:1903.03096*, 2019.
- Oriol Vinyals, Charles Blundell, Timothy Lillicrap, Daan Wierstra, et al. Matching networks for one shot learning. In *Advances in neural information processing systems*, pages 3630–3638, 2016.
- Wei-Hung Weng, Yuannan Cai, Angela Lin, Fraser Tan, and Po-Hsuan Cameron Chen. Multimodal multitask representation learning for pathology biobank

metadata prediction. *arXiv preprint arXiv:1909.07846*, 2019.

Jufeng Yang, Xiaoxiao Sun, Jie Liang, and Paul L Rosin. Clinical skin lesion diagnosis using representations inspired by dermatologist criteria. In *Proceedings of the IEEE Conference on Computer Vision and Pattern Recognition*, pages 1258–1266, 2018.

Appendix

Split	Train	Validation	Test
Patient number	9249	302	2755
Case number	11403	526	3136

Table A1: Statistics of the used dataset.

	#Class	Included classes
Common	27	Acne, Actinic Keratosis, Allergic Contact Dermatitis, Alopecia Areata, Androgenetic Alopecia, Basal Cell Carcinoma, Cyst, Eczema, Folliculitis, Hidradenitis, Lentigo, Melanocytic Nevus, Melanoma, Other, Post Inflammatory Hyperpigmentation, Psoriasis, Squamous cell carcinoma/squamous cell carcinoma in situ (SCC/SCCIS), seborrheic keratosis/irritated seborrheic keratosis (SK/ISK), Scar Condition, Seborrheic Dermatitis, Skin Tag, Stasis Dermatitis, Tinea, Tinea Versicolor, Urticaria, Verruca vulgaris, Vitiligo
Rare	42	Abscess, Acanthosis nigricans, Acne keloidalis, Amyloidosis of skin, Central centrifugal cicatricial alopecia, Condyloma acuminatum, Confluent and reticulate papillomatosis, Cutaneous lupus, Dermatofibroma, Dissecting cellulitis of scalp, Drug Rash, Erythema nodosum, Folliculitis decalvans, Granuloma annulare, Hemangioma, Herpes Simplex, Herpes Zoster, Idiopathic guttate hypomelanosis, Inflicted skin lesions, Insect Bite, Intertrigo, Irritant Contact Dermatitis, Keratosis pilaris, Lichen Simplex Chronicus (LSC), Lichen planus/lichenoid eruption, Lichen sclerosus, Lipoma, Melasma, Milia, Molluscum Contagiosum, Onychomycosis, Paronychia, Perioral Dermatitis, Photodermatitis, Pigmented purpuric eruption, Pityriasis rosea, Prurigo nodularis, Pyogenic granuloma, Rosacea, Scabies, Telogen effluvium, Xerosis

Table A2: Detailed categorization for common and rare skin conditions in the study.

Method	Train Eval	5-way-5-shot 5-way-5-shot	10-way-5-shot 5-way-5-shot	14-way-5-shot 5-way-5-shot	14-way-9-shot 5-way-5-shot
k-NN		0.544±0.010	0.55±0.010	0.548±0.010	0.545±0.010
Baseline++		0.475±0.010	0.469±0.010	0.593±0.010	0.488±0.010
Matching networks		0.597±0.010	0.592±0.010	0.566±0.010	0.581±0.010
Prototypical networks		0.587±0.010	0.613±0.010	0.610±0.010	0.605±0.010
Relation networks		0.585±0.010	0.586±0.010	0.578±0.010	0.559±0.010
MAML		0.585±0.010	0.594±0.010	0.587±0.010	0.580±0.010
Proto-MAML		0.599±0.010	0.628±0.010	0.626±0.010	0.595±0.010

Table A3: Standard FSL evaluation for the skin dataset with the change of N and k value (5-way-5-shot accuracy, with 95% confidence interval). “14-way-9-shot” indicates that we use 14-way-9-shot for the training in meta-learning, but use 5-way-5-shot for all evaluations. The boldface values indicate the best setting for each FSL algorithm.

Method	5-way-5-shot	10-way-5-shot	14-way-5-shot	14-way-9-shot
k-NN	0.137 (0.094/0.168)	0.134 (0.098/0.159)	0.117 (0.101/0.125)	0.136 (0.093/0.161)
Baseline++	0.048 (0.044/0.052)	0.050 (0.044/0.055)	0.042 (0.041/0.044)	0.049 (0.039/0.056)
Matching networks	0.235 (0.097/0.325)	0.228 (0.135/0.302)	0.229 (0.118/0.304)	0.264 (0.130/0.350)
Prototypical networks	0.211 (0.159/0.244)	0.219 (0.157/0.262)	0.219 (0.159/0.261)	0.213 (0.168/0.245)
Relation networks	0.038 (0.026/0.046)	0.056 (0.036/0.071)	0.090 (0.047/0.119)	0.072 (0.045/0.091)
MAML	0.078 (0.042/0.101)	0.181 (0.056/0.250)	0.157 (0.065/0.218)	0.210 (0.080/0.296)
Proto-MAML	0.123 (0.089/0.146)	0.184 (0.107/0.237)	0.213 (0.122/0.274)	0.240 (0.134/0.308)

Table A4: Real-world FSL evaluation. We report the performance of models trained by different N -way- k -shot setting. The value outside the parentheses is the balanced accuracy of *ALL* classes, and the values inside the parenthesis are the balanced accuracy of common/rare classes, respectively. The boldface values indicate the best algorithm for each training setup.

	All-way accuracy	Balanced accuracy	Balanced acc. (common class)	Balanced. acc. (rare class)
FSL	0.147	0.264	0.130	0.359
CSL baseline	0.648	0.411	0.525	0.347
Upsampling	0.610	0.504	0.575	0.458
BI	0.661	0.420	0.537	0.345
IFW	0.621	0.494	0.523	0.476
BI/IFW	0.620	0.506	0.515	0.500
FL	0.657	0.429	0.530	0.364
FL/IFW	0.395	0.552	0.455	0.616

Table A5: Comparison between FSL, CSL baseline and other class imbalance techniques in the all-way classification problem under single model (non-ensemble) setting. The boldface values indicate the best method for each evaluation metric. Note that all-way accuracy is a biased metric towards common classes, as the test set is dominated with common classes.

#Model	Combination	All-way accuracy	Balanced accuracy	Balanced acc. (common class)	Balanced acc. (rare class)
2	2 FSL	0.233	0.340	0.215	0.421
	2 CSL Baseline	0.663	0.431	0.523	0.371
	FSL+CSL Baseline	0.633	0.435	0.506	0.389
	2 Upsampling	0.617	0.509	0.58	0.464
	FSL+Upsampling	0.582	0.524	0.557	0.503
4	4 FSL	0.24	0.363	0.216	0.459
	4 Upsampling	0.623	0.529	0.591	0.489
	FSL+Upsampling+BI/IFW+FL/IFW	0.582	0.558	0.541	0.569

Table A6: Comparison between ensemble FSL, CSL baseline and CSL-based class imbalance techniques in the all-way classification problem under ensemble setting. Note that all-way accuracy is a biased metric towards common classes, as the test set is dominated with common classes.